Cross-linking of ultra-high molecular weight polyethylene in the melt by means of electron beam irradiation

D. J. Dijkstra*, W. Hoogsteen and A. J. Pennings†
Laboratory of Polymer Chemistry, Nijenborgh 16, 9747 AG Groningen, The Netherlands
(Received 27 January 1988; revised 15 August 1988; accepted 16 November 1988)

Compression moulded ultra-high molecular weight polyethylene (UHMWPE) was crosslinked in the melt at 200°C by means of electron beam irradiation. Gel–sol measurements revealed gel fractions up to 100%, indicating that effectively no chain scissioning occurred. Equilibrium swelling experiments were used to calculate the crosslink and entanglement densities. These densities together with differential scanning calorimetry data indicated that entanglements are extremely mobile upon crystallization. With increasing crosslink density, a change from lamellar to micellar-like crystallization was found. Trapped entanglements and crosslinks were determined to be preferentially located outside the micellar-like crystals, leading to the conclusions that they are very mobile and migrate to the disordered domains upon crystallization.

(Keywords: UHMWPE; irradiation; crosslink; crystallization; melting point depression)

INTRODUCTION

Ultra-high molecular weight polyethylene (UHMWPE) is, at room temperature, a highly polycrystalline solid, due to the presence of topological defects rather than chain ends[1]. Instantaneous crosslinking by means of high energy irradiation at this temperature would result in a considerable amount of main-chain scissioning[2–4] and a highly inhomogeneous network, because crosslinks are formed only in the non-crystalline regions[3,5–7].

In the present study, a homogeneous network was synthesized by means of high energy irradiation in the melt, thereby improving the material properties such as impact strength, abrasion resistance[8,9] and creep[10].

It has been suggested[11] that, in order to obtain homogeneous networks, crosslinking of UHMWPE should be done at temperatures above 150°C, to avoid irregularities due to the presence of remnants of the initial solid state of polyethylene. The UHMWPE can easily be irradiated at 200°C, due to the extremely high melt viscosity, without changes in the sample dimensions.

This paper deals with the synthesis of the networks and characterization, by means of sol–gel analysis, equilibrium swelling and small angle X-ray scattering measurements together with differential scanning calorimetry.

EXPERIMENTAL

Sample preparation

The UHMWPE (Hifax 1900 from Hercules, $M_w = 4 \times 10^6\,kg\,kmol^{-1}$, $M_n = 5 \times 10^5\,kg\,kmol^{-1}$) was compression moulded at 200°C and 64 MPa for 50 h, in a nitrogen atmosphere. The samples were annealed at 200°C for two months under vacuum, in order to allow the molecules to reptate and segregate so that an equilibrium entanglement network could be formed. From the 1 mm thick sheet, bars of $1 \times 1 \times 30\,mm^3$ were cut, which were glued onto an aluminium cylinder. The cylinder was irradiated, in a nitrogen atmosphere, at 200°C with 3 MeV electrons by means of a Van de Graaff generator as described previously[4]. The samples were cooled down to room temperature at a rate of $20°C\,min^{-1}$.

Sol–gel measurements

Extraction of the sol fraction was performed with boiling *p*-xylene, containing 0.5 wt% of anti-oxidant (2,6-di-t-butyl-4-methylcresol) for 64 h. The samples were deswollen in acetone and dried under vacuum at 50°C for 24 h. The gel fractions were determined by weight.

Equilibrium swelling

Equilibrium swelling experiments were performed in *p*-xylene at 130°C. The extracted sample was swollen for 3 h, to attain equilibrium. The degree of swelling was calculated from the ratio of the weights of swollen and dry samples and the specific density of the diluent ($0.81\,kg\,dm^{-3}$) at 130°C.

Differential scanning calorimetry (d.s.c.)

The d.s.c. curves were obtained by means of a Perkin–Elmer DSC-7. Each sample, approximately 5 mg in weight, was heated at scan speeds of 2, 5, 20 and $40°C\,min^{-1}$. The end melting temperatures, calculated from the d.s.c. curves, were extrapolated to zero scanning rate.

Small angle X-ray scattering (SAXS)

SAXS measurements were carried out using a Kratky camera with entrance slits of 80 and 40 μm. The data obtained were desmeared, i.e. were corrected for the slit

* Present address: Bayer AG, Zentrale Forschung TPE 1, 5090 Leverkusen, FRG
† To whom correspondence should be addressed

0032-3861/89/050866-08$03.00

length, and Lorentz corrected with the aid of a computer program developed by Vonk[12,60].

RESULTS AND DISCUSSION

Compression moulded UHMWPE was annealed for two months at 200°C under vacuum, in order to obtain an equilibrium entanglement network. The entanglements were trapped in space by crosslinking the UHMWPE in the melt at 200°C by means of electron beam irradiation.

Sol–gel measurements revealed extremely high gel fractions, up to 100%. These measurements were analysed in terms of the Charlesby–Pinner equation[13], relating the sol fraction, s, to the irradation dose, r:

$$s+s^{1/2}=\frac{G(s)}{G(x)}+\frac{9.6\times10^5}{G(x)M_w r} \quad (1)$$

where $G(s)$ is the number of main-chain scissions and $G(x)$the number of crosslinks, both produced per 10 eV absorbed energy, and M_w is the weight average molecular weight of the initial polymer.

Equation (1) holds strictly for random molecular weight distributions, whether or not main-chain scissioning occurs simultaneously with cross-linking, and holds also at high doses for other distributions, provided that cross-linking is accompanied by scissioning. Inokuti[14] and Saito *et al.*[15] derived equations giving the sol fraction of polymer undergoing simultaneous crosslinking and scissioning for various molecular size distributions, leading to a convex curve in the Charlesby–Pinner plot for the polydisperse UHMWPE used in this study.

Extrapolation of the Charlesby–Pinner plot (see *Figure 1*) to infinite irradiation dose yielded a $G(s)/G(x)$ value of zero. We can explain this value by assuming either that no main-chain scissioning occurred, or that the radicals, formed by the scissioning, recombine in a cage reaction, because of the extremely high melt viscosity, analogous to the cage reaction in crystalline polyethylene[5].

The equilibrium degree of swelling (see *Figure 2*), q, was used to calculate the effective network chain density, v, using the swelling theory of Flory[16]. Flory treated the elastic contribution to the chemical potential of the diluent in a swollen network by taking into account the effect of constraints on the junctions in a real network.

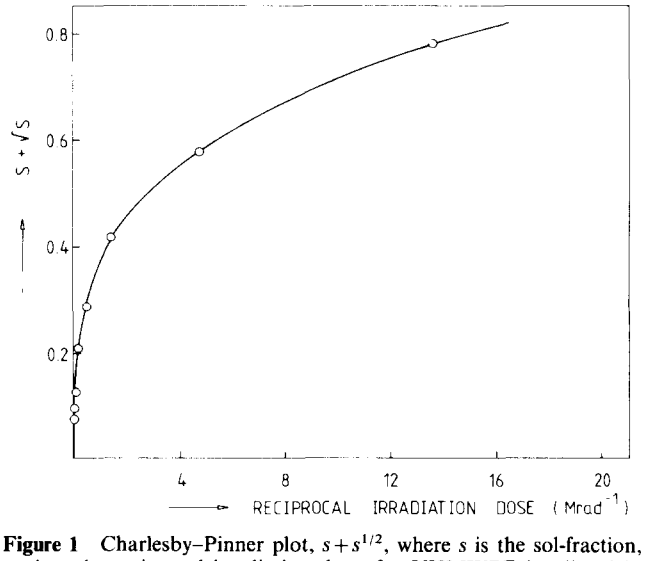

Figure 1 Charlesby–Pinner plot, $s+s^{1/2}$, where s is the sol-fraction, against the reciprocal irradiation dose, for UHMWPE irradiated in the melt at 200°C

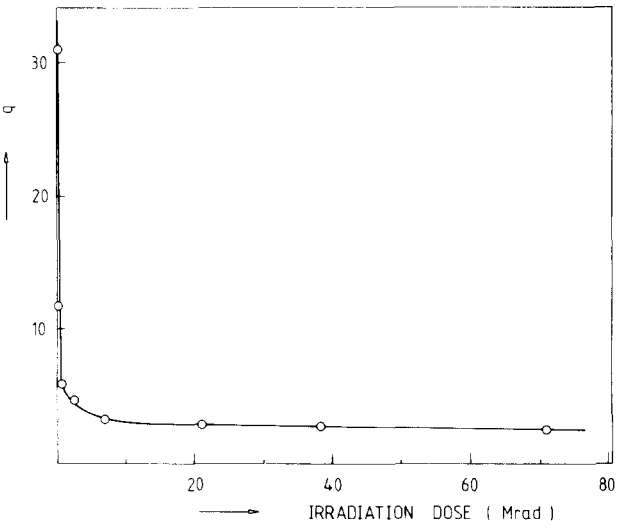

Figure 2 Degree of equilibrium swelling, in *p*-xylene at 130°C, *versus* the irradiation dose

From this theory the following formula for the effective network chain density, v (in kmol dm^{-3}), was deduced[17]

$$v=-\frac{\ln(1-q^{-1})+q^{-1}+\chi q^{-2}}{F_\phi V_1 q_0^{-2/3} q^{-1/3}} \quad (2)$$

where χ is the Flory–Huggins interaction parameter, and V_1 represents the partial molar volume of the swelling medium. The factor F_ϕ characterizes the extent to which the deformation in swelling approaches the affine limit[18]. For affine deformation, $F_\phi=1$. In all other cases the theoretical values of F_ϕ are given by[17]

$$F_\phi=(1-2/\phi)[1+(\mu/\xi)K] \quad (3)$$

in which μ represents the number of junctions in the network. For a perfect ϕ-functional network, $\mu/\xi=2/(\phi-2)$. The quantity K is a function of q and also of two network parameters κ and p which specify, respectively, the constraints on the crosslinks from the neighbouring junctions and the dependence of the crosslink fluctuations on the strain. As the deviation of a real network from the phantom network behaviour becomes more significant, there will be an increase in both parameters κ and p. Since the swelling measurements were conducted in *p*-xylene at 130°C, the Flory–Huggins interaction parameter can be written as $\chi=0.33+0.55q^{-1}$ (Reference 19), while V_1 was assumed to be 136 dm^3 kmol^{-1}. Since K is a function of q and the parameters κ and p, this implies that K is a function of the temperature and of the polymer–solvent system under consideration. Flory[16] showed that to a first approximation $\kappa=20$ and $p=2$ are reasonable estimates. K can now be derived from Figure 1 of Reference 16. Finally, it is assumed that the crosslinks were all tetra-functional. The results of the calculations of the effective network chain density are presented in *Figure 3*.

The intercept on the v-axis in *Figure 3*, obtained by extrapolation of the linear part of the curve to zero dose, corresponds to twice the entanglement concentration in the network[11,20,21]. From the intercept a molecular weight between entanglements of 4700 kg kmol^{-1} was calculated. The equilibrium number average molecular weight between entanglements is considered to be about 2000 kg kmol^{-1} (refs 22–24). The reason for this small discrepancy in the molecular weight between entangle-

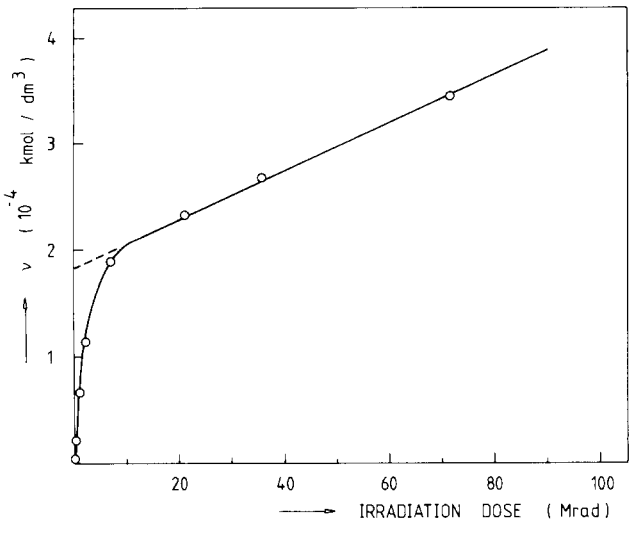

Figure 3 Effective network chain density, calculated from the equilibrium degree of swelling, *versus* the irradiation dose. The intersection of the extrapolated linear part of the curve with the effective network chain density axis equals twice the entanglement density

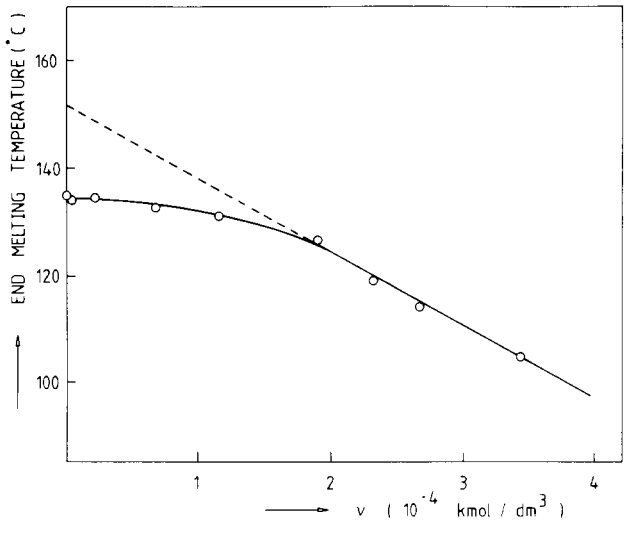

Figure 4 End melting temperature, extrapolated to zero scan speed, *versus* the effective network chain density, ν, calculated from the equilibrium degree of swelling

ments might be the fact that the swelling diluent used is not an extremely good solvent. Additionally, many entanglements might slip off[25], instead of being pulled taut, and give a smaller contribution to the elasticity part of equation (2). Another reason might be the possibility that, even after two months of annealing in the melt, the entanglement network is still not in a state of equilibrium.

From the slope of the linear part of *Figure 3*, the number of crosslinks created upon irradiation of the polyethylene in the melt per 10 eV absorbed energy was calculated to be $G(x)=2.6$, in very good agreement with the literature[19,26]. This value of $G(x)$ together with the data points in *Figure 1* shows that no, or only very little, thermal degradation occurred during annealing of the samples for two months at 200°C.

In *Figure 4* the end melting temperature is plotted against the effective network chain density, ν. The effective network chain density is not corrected for the entanglement concentration. As will be shown later in this paper, the entanglements are transported to the fold surfaces upon crystallization, thereby giving almost no contribution to the melting point depression. Trapped entanglements, however, are more sessile and are expected to contribute to the melting point depression. Extrapolation of the end melting temperature to zero effective network chain density, i.e. polyethylene without crosslinks or trapped entanglements, yielded an end melting temperature of 152°C, a temperature several degrees too high compared with the value found by Wunderlich and Czorny[27], who found $T_m^\circ = 141.5 \pm 0.5$°C for the equilibrium melting temperature for polyethylene. In *Figure 5* the heat of fusion is plotted against the effective network chain density.

The long period found by means of SAXS measurements together with the heat of fusion, i.e. the crystallinity of the samples, were used to calculate the crystal length, l_c, shown in *Table 1*, by means of

$$l_c = (C\rho_a L)/(C\rho_a + (1-C)\rho_c)$$

where $\rho_a = 0.855\,\mathrm{kg\,dm^{-3}}$ and $\rho_c = 1.0\,\mathrm{kg\,dm^{-3}}$ are the specific densities of the amorphous and crystalline polymer respectively. The crystallinity as calculated from the heat of fusion is represented by $C = \Delta H_f/\Delta H_f^0$, where $\Delta H_f^0 = 292\,\mathrm{J\,g^{-1}}$ is the heat of fusion of the ideal polyethylene crystal[27].

Table 1 Network characteristics of ultra-high molecular weight polyethylene crosslinked in the dry state at 200°C by means of electron beam irradiation

R^a (Mrad)	ν^b (mol dm^{-3})	L^c (nm)	l^d_{cryst} (nm)	$l^e_{contour}$ (nm)	T^f_{end} (°C)	ΔH^g_f (J g^{-1})	q^h	g^i (%)
0	–	42	19	–	134.9	161	–	0
0.07	0.004	43	20	1820	134.1	148	30.3	73.3
0.21	0.022	43	20	354	134.6	146	11.8	82.9
0.71	0.067	42	19	115	132.4	151	6.0	89.9
2.1	0.116	38	17	67	131.4	151	4.4	94.6
7.1	0.190	27	12	41	126.5	136	3.3	96.8
21	0.232	20	8	33	119.1	124	3.0	98.6
36	0.268	17	6	29	114.0	121	2.7	99.1
71	0.344	14	4	23	105.1	94	2.4	99.4

[a] Irradiation dose
[b] Effective network chain density
[c] Long period of SAXS measurements
[d] Crystal length, calculated from the long period and crystallinity
[e] Contour length between crosslinks/trapped entanglements
[f] Heat of fusion
[h] Equilibrium degree of swelling
[i] Gel fraction

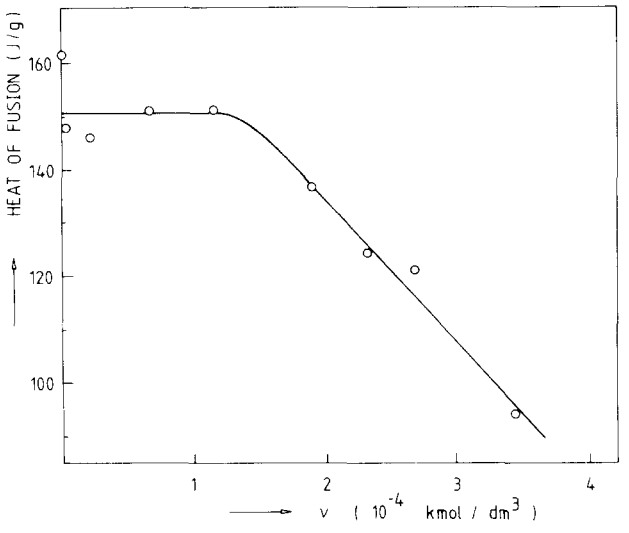

Figure 5 Heat of fusion, from differential scanning calorimetry, *versus* the effective network chain density, v, calculated from the equilibrium degree of swelling

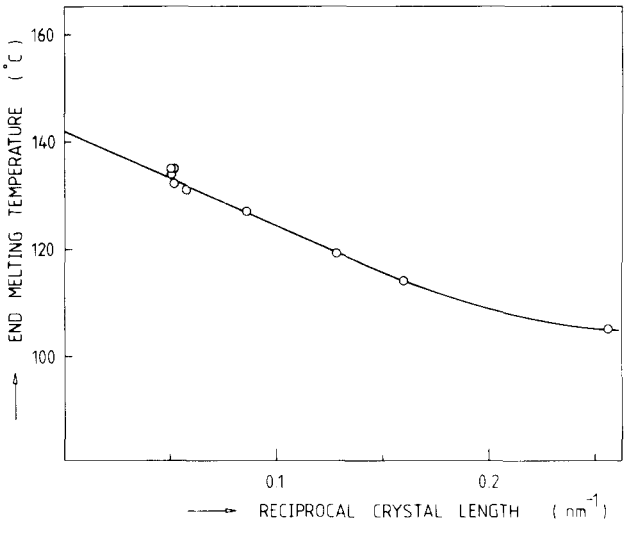

Figure 6 End melting temperature, extrapolated to zero scan speed, *versus* the reciprocal crystal length, calculated from small angle X-ray scattering

In *Figure 6* the end melting temperature is plotted against the reciprocal crystal length. Extrapolation of the end melting temperature to infinite crystal length yielded an end melting temperature of 142°C, in agreement the equilibrium melting temperature reported by Wunderlich and Czorny[27]. The data in *Figure 6* can be described by the well known Gibbs–Thomson relationship (equation (5), below)[28,29]. It follows directly from Flory's theory of the thermodynamics of crystallization and melting of semi-crystalline polymers that, if the crystallite length does not attain its equilibrium value, the relationship between the melting temperature and the crystallite thickness, l_c, of the lamellae is given to a first approximation by the Gibbs–Thomson equation[31]

$$T_m = T_m^0\left(1 - \frac{2\sigma_e v_p^c}{\Delta H_f l_c} - \frac{4\sigma_s v_p^c}{\Delta H_f D}\right) \quad (5)$$

where T_m^0 is the melting temperature of an ideal polyethylene crystal of infinite size, l_c is the length of the crystalline, D is the lateral dimension of the crystallite, σ_e is the surface free energy of the (001) plane, σ_s is the free energy of the lateral surfaces, v_p^c is the specific volume, and ΔH_f is the heat of fusion. With the parameters $\sigma_e \approx 0.1\,J\,m^{-2}$ (refs 32–36), $\sigma_s \approx 0.01\,J\,m^{-2}$ (ref. 37), $\Delta H_f = 2.92 \times 10^5\,J\,kg^{-1}$ (ref. 27) and $v_p^c = 1.035 \times 10^{-3}\,m^3\,kg^{-1}$.

The Gibbs–Thomson equation gives us a way to evaluate the melting temperature of small crystals. The major difficulty in using equation (5) is the instability of small crystals. Typically, small lamellae will anneal on heating to the melting temperature and give a higher experimental melting temperature of a perfect crystal. From *Figure 7*, it is evident that no crystal thickening occurs; on the contrary, superheating is recorded. At high irradiation doses, the annealing is hindered by the crosslinks, a phenomenon which is well known from the literature[38,39]. But even the non-irradiated lamellarly crystallized sample displays no crystal thickening upon annealing. This again indicates that the entanglements are located at the fold surfaces and inhibit the annealing of the polymer crystals so that zero entropy production melting can be achieved[40].

The data in *Figure 6* can be fitted by equation (5) by the substitution of $\sigma_e = 0.06\,J\,m^{-2}$ for the interfacial free energy per unit of area at the crystallite ends, a value smaller than quoted above, but almost equal to the one found in Reference 41. The second term in equation (5) seems to have no influence on the melting temperature, as the extrapolation, shown in *Figure 6*, yields a value close to the equilibrium melting temperature, although the extrapolation to infinite crystal length is performed in only one direction. This is not surprising, because the free energy of the lateral surfaces, σ_s, is much lower than the surface free energy of the (001) plane.

Arakawa and Nagotoshi[42,43] showed that extrapolation of the melting temperature of nylon-6 to the specific volume of the idealized crystal, i.e. crystal without lattice distortions, led to a value higher than the value obtained by extrapolation of the reciprocal crystallite size. This effect may have been compensated for by superheating for the experiments presented in this paper.

In his theory on the thermodynamics of crystallization, Flory[30] also deduced a melting point depression equation

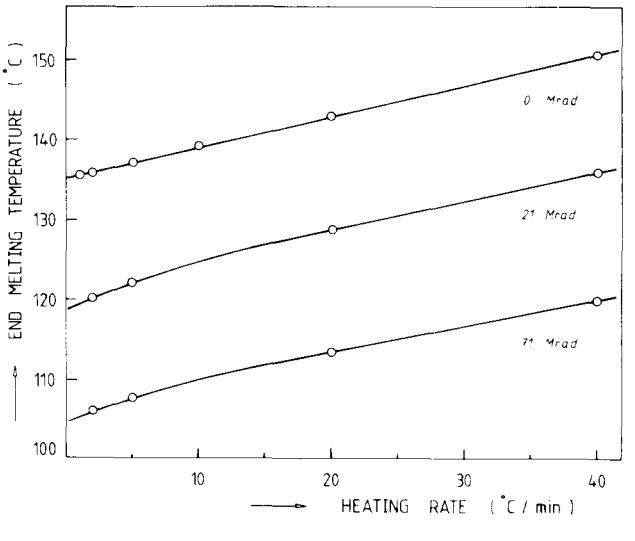

Figure 7 End melting temperature, as recorded from differential scanning calorimetry, *versus* the heating rate. No crystal thickening can be observed

for random copolymers. In this theory, a linear copolymer was considered composed of units of type A capable of crystallizing and other units, B, incapable of occupying the lattice characteristic of A, with the two types of units occurring in random sequence.

After a few modifications[44,45] this theory gives the following expression:

$$\frac{1}{T_m}-\frac{1}{T_m^0}=\frac{R}{\Delta H_f}(\alpha v_c+\beta v_m+\gamma v_1+2\delta\varepsilon) \qquad (6)$$

where T_m is the melting point of the polymer, T_m^0 the equilibrium melting point of the polymer without defects, R the gas constant equals $8.3143\,J\,K^{-1}\,mol^{-1}$, ΔH_f the heat of fusion per unit volume is $2.5\times10^5\,J\,dm^{-3}$ (refs 27, 46), v_c is the concentration of intermolecular crosslinked units, v_i the concentration of intramolecular crosslinked units, v_m the concentration of chemical modified units and ε the entanglements concentration. Finally α, β, γ and δ are the weight factors for the different kinds of chain units in the equation, i.e. the number of chain units excluded from crystallization per crosslink or entanglement.

Since the number of chains, n, within the domain of one radius of gyration, R_g, is given by

$$n=\tfrac{4}{3}\pi R_g^3/Nv \qquad (7)$$

where N is the number of units per chain and v the volume per chain unit, and in the melt the radius of gyration scales as $N^{0.5}$, i.e n scales as $N^{0.5}$, it is clear that the contribution of intramolecular crosslinks may be neglected in equation (6) for the ultra-high molecular weight polyethylene used.

Both crosslink density and concentration of chemical modified units are proportional to the irradiation dose. The most frequently observed chemical modification is the *trans*-vinylene group[5]. The effect of *trans*-vinylene groups on the melting point depression is expected to be small compared with the contribution of crosslinks, because the vinylene group can be incorporated in the crystal[5,47].

The melting point depression plotted against the effective network chain density is shown in *Figure 8*. For low effective network chain densities an almost constant melting point depression was found, whereas at higher effective network chain densities the melting point depression increases linearly. In *Figure 8(a)* the melting point depression for $T_m^0=142°C$ is shown. The linear part of the melting point depression at high irradiation doses does not extrapolate to the origin, because a large fraction of trapped entanglements do not contribute to the melting point depression, because they are able to move, especially at low irradiation doses. For *Figure 8(b)* a value of $T_m^0=152°C$ is used, the value extrapolated from *Figure 4*. It is trivial that the linear part extrapolates to the origin in *Figure 8(b)*. As stated above, the effective network chain density is too high compared with the melting point depression, i.e. in *Figure 4* the fraction of trapped entanglements not involved in the melting point depression, because of their high mobility, should be subtracted from the effective network chain density. This cannot be performed easily, because the mobility of the entanglements decreases as the number of crosslinks increases. But it is evident that a decrease in effective network chain density in *Figure 4* should yield a decreased extrapolated melting temperature.

Since Keller made his chain-folding postulate in 1957,

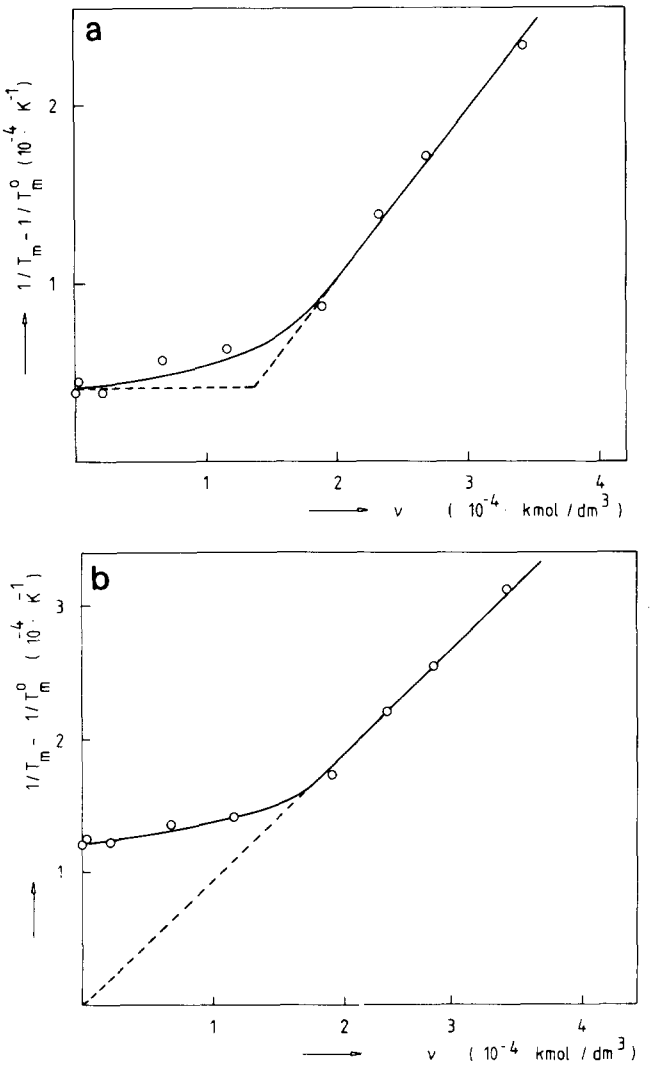

Figure 8 Melting point depression plotted as a function of the effective network chain density for (a) $T_m^0=142°C$ and (b) $T_m^0=152°C$

it has been well known that polyethylene crystallizes in a folded chain lamellar morphology (see, e.g., Reference 48 for a review). Due to the high cooling rate, the ultra-high molecular weight of the polyethylene and the presence of entanglements, one molecule crystallizes into several lamellae leading to Fischer's 'Erstarrungs modell'[49–51]. The high cooling rate prevents the chain from disentangling, but the entanglements can move over considerable distances[25]. The mobility of the entanglements is greatly reduced by the introduction of chemical crosslinks upon irradiation. The entanglements are trapped by the chemical crosslinks and become sessile.

In *Figure 4* an almost constant melting point is found for low values of the effective network chain density, i.e. for a small number of trapped entanglements and crosslinks. Above an effective network chain density of $v\approx0.14\,mol\,dm^{-3}$, the melting point starts to decrease. In *Figure 5*, the same effect is observed for the heat of fusion of the irradiated samples. In *Figure 8* an almost constant melting point depression is observed up to $v\approx0.14\,mol\,dm^{-3}$; above this v-value a linear increase of the melting point depression is observed. The change in the melting point depression, the melting point and the heat of fusion can be explained by a change in morphology upon crystallization. As mentioned above, polyethylene

crystallizes into lamellae, but at a certain crosslink or trapped-entanglement concentration, lamellar crystallization can no longer occur, because the contour length between the crosslinks or entanglements has become less than the fold length of the lamellae. From *Table 1* one can see that the contour length of the chains between trapped entanglements or crosslinks almost equals the fold length, i.e. the crystal length ($l_c \approx 20$ nm) of the samples with low irradiation doses, at an effective network chain density of $\nu \approx 0.19$ mol dm^{-3}.

The change in morphology upon crystallization was earlier reported by Gielenz and Jungnickel[54], who showed that highly crosslinked linear polyethylene crystallizes in a micellar-like way.

In the first data point of the linear part of *Figure 8*, the number of crosslinks consists almost entirely of trapped entanglements (compare *Figure 3*), i.e. the trapped entanglements give the same contribution to the melting point depression as chemical crosslinks do. From the slope of the linear part of *Figure 8* the number of chain units excluded from crystallization per crosslink or trapped entanglement were calculated to be $\alpha \approx \delta \approx 26$. But from the melting point depression of the non-crosslinked polyethylene, completely due to the presence of entanglements, a δ-value of 6 for $T_m^0 = 142$°C was calculated, i.e. the contribution to the melting point depression per trapped entanglement is much larger than the contribution per free entanglement. This difference in weight factor elucidates the enormous mobility of the free entanglements in the non-crosslinked polyethylene during crystallization.

The number of chain units excluded from crystallization as calculated from the melting point depression should correspond to the difference in the heat of fusion, measured by thermal analysis.

The actual number of units excluded from crystallization was calculated from the slope of the linear part of *Figure 5* to be $\alpha \approx 58$, about twice the value calculated from the melting point depression. The large difference between the calculated α-value from Flory's melting point model is not surprising, because in this model the chain units excluded from crystallization are thought to be able to attain the random coil conformation, i.e. maximum entropy. From the differences in contour length of the chains between crosslinks or trapped entanglements, the long period and the crystal length, presented in *Table 1*, it is evident that for the highly irradiated samples the contour length is by far too short to cross the amorphous domains, while performing a random walk. In *Figure 9* this is schematically draw for the sample irradiated at a dose of 21 Mrad (long period $L \approx 20$ nm, crystal length $l_c \approx 8$ nm, contour length $l \approx 33$nm). Summarizing, we can say that crosslinking of UHMWPE changes the crystallization considerably. At low crosslink densities, already a large fraction of entanglements has become trapped.

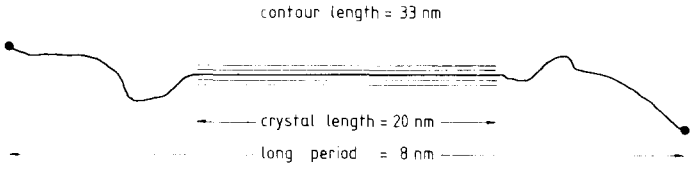

Figure 9 Schematic drawing of a polyethylene chain, partly embedded in a micellar like crystal, between two crosslinks or trapped entanglements, for UHMWPE irradiated in the melt at 200°C with an irradiation dose of 21 Mrad

Table 2 Calculated volume of polymer per randomly distributed crosslink or trapped entanglement

R^a (Mrad)	ν^b (mol dm^{-3})	V^c (nm^3)
0.07	0.004	833
0.21	0.022	152
0.71	0.067	50
2.1	0.116	29
7.1	0.190	17.5
21	0.232	14.4
36	0.268	12.4
71	0.344	9.7

[a] Irradiation dose
[b] Effective network chain density
[c] Calculated volume per randomly distributed crosslink/trapped entanglement

These trapped entanglements are still very mobile and it is likely that they move to the folds containing domains upon crystallization. In the melt, the lamellar fold length in UHMWPE is about half the equilibrium contour length between entanglements in the melt, i.e. every fold should contain about two entanglements. Lacher *et al.*[55,56] have calculated that entanglements involving chains that re-enter the same crystalline layer, may contribute at least as much to the interconnection of crystal lamellae in some polymers as tie molecules do[57].

With an increasing number of crosslinks, the trapped entanglements become less and less mobile. When the contour length between trapped entanglements and crosslinks has become less than twice the lamellar fold length, it is likely that the crystallization form changes from lamellar to micellar-like. These micellar-like crystals should on the one hand display superheating, because the chain ends are more or less fixed in space by means of the crosslinks, i.e. the chains cannot attain a random coil upon melting[58], and on the other hand a melting temperature lower than that of an ideal polyethylene crystal, because they have finite dimensions.

In *Table 2* the average volumes of polymer per trapped entanglement and crosslink, calculated from the effective network chain density assuming that the trapped entanglements and the crosslinks are homogeneously distributed in space, are shown. These volumes are unrealistically small compared with the crystal lengths, see *Table 1*, and the lateral crystal dimensions as calculated from the Gibbs–Thomson relationship applied to *Figure 6*, leading to the conclusion that either the crosslinks and trapped entanglements in highly crosslinked polyethylene become inhomogeneously distributed in space upon crystallization, due to migration to the disordered domains, or that a considerable number of them are incorporated in the crystallites. Guiu and Shadrake[59] have formulated an elastic model of a crosslink between adjacent molecules in a polyethylene crystal. The displacements of chain units near the crosslink, they calculated, are not large enough to explain the number of chain units excluded from crystallization ($\alpha \approx 58$) found in this study, i.e. it seems likely that a large number of the crosslinks and trapped entanglements are displaced outside the crystals upon crystallization.

In *Figure 10*, some of the differential scanning calorimetry curves are shown. The peak width decreases with increasing irradiation dose, i.e. the distribution of crystal dimensions decreases with increasing irradiation dose. In *Figure 11* the small angle X-ray scattering curves are

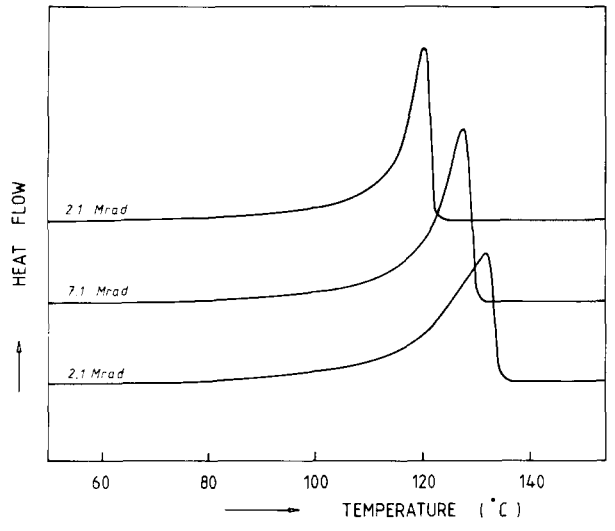

Figure 10 Differential scanning calorimetry curves, taken at a scan speed of 5°C min^{-1}, for samples irradiated at 200°C with dosages of 2.1, 7.1 and 21 Mrad. The d.s.c. peaks do not broaden with increasing irradiation dose

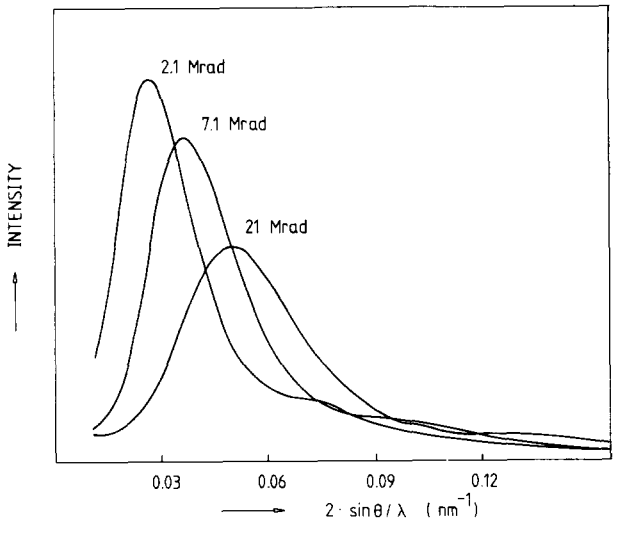

Figure 11 Small angle X-ray scattering curves for samples irradiated at 200°C with dosages of 2.1, 7.1 and 21 Mrad. The SAXS maxima broaden with increasing irradiation dose

shown for the same samples shown in *Figure 10*. In *Figure 11* an enormous broadening of the SAXS curves is recorded with increasing irradiation dose. Because of the results of *Figure 10*, it is likely that the broadening of the SAXS curves is not due to the distribution of crystallite dimensions in the samples. A maximum in the SAXS curve means that there is a local orientation in the samples. For samples with lamellar crystallization, local orientation (i.e. stacked lamellae) is the only possibility for attaining high crystallinity. From *Figure 11* we surely may conclude that there is still local orientation for the micellar-like crystallization, although it might not be as pronounced as it is for stacked lamellar crystallization.

CONCLUSIONS

The following conclusions may be drawn from the present study on the crosslinking of ultra-high molecular weight polyethylene in the melt at 200°C by means of electron beam irradiation.

Since sol–gel measurements revealed extremely high gel fraction, up to 100%, one is led to the conclusion that no chain scissioning occurs upon irradiation or that the radicals formed recombine in a cage reaction. From the equilibrium swelling experiments in *p*-xylene a molecular weight between the entanglements in the melt of 4700 kg kmol^{-1} was calculated. This value is probably a factor of two too high, which is possibly due to the limited degree of swelling of the polyethylene network in *p*-xylene and the sliding motion of the entanglements. Extrapolation of the end melting temperature to infinite crystal length in the chain direction yields a value of $T_m = 142$°C.

Differential thermal analysis of the UHMWPE networks revealed that the number of chain-units excluded from crystallization is much larger for trapped entanglements and chemical crosslinks than for free entanglements, probably due to the high mobility of the free entanglements.

From the increase of the effective network chain density, calculated from the equilibrium swelling experiments, a value for $G(x)$ of 2.6, the number of crosslinks formed per 100 eV absorbed energy, was calculated.

From the differential thermal analysis data a change in crystal morphology from lamellar to micellar-like crystallization was deduced for highly irradiated samples. The high mobility of the free entanglements enables the non-crosslinked polyethylene chain to transport entanglements outside the lamellae. When these entanglements become trapped by crosslinks, this transport is no longer possible. Differential thermal analysis and equilibrium swelling experiments showed that lamellar crystallization occurs when the contour length between the trapped entanglements or crosslinks is larger than twice the fold length of the lamellar crystal. Chains with contour lengths between crosslinks or trapped entanglements smaller than twice the fold length of the lamella undergo micellar-like crystallization.

The volume of polymer per crosslink and trapped entanglement, calculated from the effective network chain density, yields values very much smaller than the dimensions calculated from the small angle X-ray scattering measurements and from the Gibbs–Thomson relationship, indicating that the crosslinks and trapped entanglements are not homogeneously distributed upon crystallization. Since they were introduced homogeneously, because of the instantaneous crosslinking, due to the very high irradiation dose rate, these crosslinks and trapped entanglements are thought to migrate away from the growth front, and will have to be very mobile.

ACKNOWLEDGEMENTS

The authors would like to thank Prof. A. Hummel, Dr L. H. Luthjens, M. L. Hom and M. J. W. Vermeulen of the Interuniversitair Reactor Instituut at Delft in the Netherlands for their permission and assistance in using the Van de Graaff accelerator for the irradiation experiments. This study was supported by the Netherlands Foundation for Chemical Research (S.O.N.) with financial aid from the Netherlands organization for scientific research (N.W.O.).

REFERENCES

1 Fatou, J. G. and Mandelkern, L. *J. Phys. Chem.* 1965, **69**, 417
2 Shinde, A. and Salovey, R. *J. Polym. Sci., Polym. Phys. Edn.* 1985, **23**, 1681
3 Batateja, S. K., Andrews, E. H. and Young, R. J. *J. Polym. Sci., Polym. Phys. Edn.* 1983, **21**, 523
4 Dijkstra, D. J. and Pennings, A. J. *Polym. Bull.* 1987, **17**, 507
5 Ungar, G. *J. Mater. Sci.* 1981, **16**, 2635
6 Keller, A. 'Developments in Crystalline Polymers 1' (Ed. D. C. Bassett), Applied Science Publishers, London, p. 37
7 Dole, M. *Polym. Plast. Technol. Eng.* 1979, **13**(1), 41
8 Atkinson, J. R. and Sonie, A. W. 'Proc. 5th Int. Conf. Polym. Med. Surg.', Holland, 1986, p. 411
9 Jones, W. R. Jr and Hady, W. F. *Wear* 1981, **70**, 77
10 Klein, P. G., Ladizesky, N. H. and Ward, I. M. *J. Polym. Sci., Polym. Phys. Edn.* 1986, **24**, 1093
11 de Boer, J. and Pennings, A. J. *Makromol. Chem. Rapid Commun.* 1981, **2**, 749
12 Vonk, C. G. *J. Appl. Cryst.* 1971, **4**, 340
13 Charlesby, A. and Pinner, S. H. *Proc. R. Soc. Lond.* 1959, **A249**, 367
14 Inokuti, M. *J. Chem. Phys.* 1963, **38**, 2999
15 Saito, O., Kang, H. Y. and Dole, M. *J. Chem. Phys.* 1967, **46**, 3607
16 Flory, P. J. *Macromolecules* 1979 **12**, 119
17 Lorente, M. A. and Mark, J. E. *Macromolecules* 1980, **13**, 681
18 Mark, J. E. *Pure Appl. Chem.* 1981, **53**, 1495
19 Gent, A. N. and Vickroy, V. V. Jr *J. Polym. Sci. A-2* 1967, **5**, 47
20 de Boer, J. and Pennings, A. J. *Polymer* 1982, **23**, 1944
21 Ferry, J. D. 'Viscoelastic Properties of Polymers', 3rd Edn, Wiley, New York, 1980, p. 408
22 Porter, R. S. and Johnson, J. F. *Chem. Rev.* 1966, **66**, 1
23 Greasley, W. W. *Adv. Polym. Sci.* 1974, **16**, 55
24 Posthuma de Boer, A. and Pennings, A. J. *J. Polym. Sci., Polym. Phys. Edn.* 1976, **14**, 187
25 Ball, R. C., Doi, M., Edwards, S. F. and Warner, M. *Polymer* 1981, **22**, 1010
26 Chapiro, A. 'Radiation Chemistry of Polymeric Systems', Interscience, New York, 1962, p. 430
27 Wunderlich, B. and Czorny, G. *Macromolecules* 1977, **10**, 906
28 Weeks, N. E. and Porter, R. S. *J. Polym. Sci., Polym. Phys. Edn.* 1975, **13**, 2049
29 Gell, P. H. 'Polymer Single Crystals', Interscience, New York, 1963
30 Flory, P. J. *J. Chem. Phys.* 1949, **17**, 223
31 Mandelkern, L. 'Crystallization of Polymers', McGraw-Hill Inc., New York, 1964, p. 33
32 Flory, P. J. and Vrij, A. *J. Am. Chem. Soc.* 1963, **85**, 3548
33 Mandelkern, L., Posner, A. S., Diorio, A. F. and Roberts, D. E. *J. Appl. Phys.* 1961, **32**, 1509
34 Bear, R. S. *J. Am. Chem. Soc.* 1944, **66**, 1297
35 Richardson, M., Flory, P. J. and Jackson, J. B. *Polymer* 1963, **4**, 221
36 Cormia, R. L., Prince, F. P. and Turnbull, D. *J. Chem. Phys.* 1962, **37**, 1333
37 Turnbull, D. and Cormia, R. L. *J. Chem. Phys.* 1961, **34**, 820
38 Salovey, R. and Bassett, D. C. *J. Appl. Phys.* 1964, **35**, 3216
39 Bair, H. E. and Salovey, R. *J. Polym. Sci., Polym. Lett. Edn.* 1967, **5**, 429
40 Wunderlich, B. 'Macromolecular Physics', vol. 3, Academic Press, New York, 1980, p. 30
41 Jackson, J. B., Flory, P. J. and Chiang, R. *Trans. Faraday Soc.* 1963, **59**, 1906
42 Arakawa, T., Nagatoshi, F. and Arai, N. *J. Polym. Sci. A-2* 1969, **7**, 1461
43 Arakawa, T. and Nagotoshi, F. *J. Polym. Sci., Polym. Lett. Edn.* 1970, **8**, 41
44 Posthuma de Boer, A. and Pennings, A. J. *Faraday Disc. Chem. Soc.* 1979, **68**, 345
45 Akana, Y. and Stein, R. S. *J. Polym. Sci., Polym. Phys. Edn.* 1975, **13**, 2195
46 Pennings, A. J. and Zwijnenburg, A. *J. Polym. Sci., Polym. Phys. Edn.* 1979, **17**, 1011
47 Glenz, W., Kilian, H. G. and Mueller, F. H. *Coll. Polym. Sci.* 1966, **206**, 37
48 Keller, A. *Rep. Prog. Phys.* 1968, **31**, 623
49 Fischer, E. W. *Pure Appl. Chem.* 1978, **50**, 1319
50 Fischer, E. W., Stamm, M., Dettenmaier, M. and Herchenröder, P. *Am. Chem. Soc. Pol. Prepr.* 1979, **20**, 1, 219
51 Stamm, M., Dettenmaier, M., Herchenröder, P., Fischer, E. W. and Haas, J. 'Europhys. Conf. Abstr.', 1978, 2F, C7
52 Fischer, E. W. 'Europhys. Conf. Abstr.', 1977, 2E, 71
53 Stamm, M., Fischer, E. W., Dettenmaier, M. and Convert, P. *Faraday Discuss. R. Soc. Chem.* 1979, **68**, 263
54 Gielenz, G. and Jungnickel, B.-J. *Coll. Polym. Sci.* 1982, **260**, 742
55 Lacher, R. C., Bryant, J. L., Howard, L. N. and Sumners, D. W. *Macromolecules* 1986, **19**, 2639
56 Lacher, R. C. Supercomputer Computations Research Institute, Florida State University, Tallahassee, USA, FSU-SCRI-87-20, 1987
57 Mandelkern, L. *J. Polym. Sci. C* 1966, **15**, 129
58 Elyashevich, G. K., Litvina, T. G. and Baranov, V. G. *Acta Polym.* 1983, **34**, 390
59 Guiu, F. and Shadrake, L. G. *Proc. R. Soc. Lond.* 1975, **A346**, 305
60 Vonk, C. G. *Makromol. Chem., Macromol. Symp.* 1988, **15**, 215